VOL. 28 NO. 5 Chinese Meteorological Society 90th Anniversary Special Collection 2014

Research Progress in China on the Tropical Atmospheric Intraseasonal Oscillation

LI Chongyin[1,2] (李崇银), LING Jian[1*] (凌 健), SONG Jie[1] (宋 洁), PAN Jing[1] (潘 静), TIAN Hua[1] (田 华), and CHEN Xiong[2] (陈 雄)

1 *State Key Laboratory of Numerical Modeling for Atmospheric Sciences and Geophysical Fluid Dynamics, Institute of Atmospheric Physics, Chinese Academy of Sciences, Beijing* 100029

2 *Institute of Meteorology and Oceanography, PLA University of Science and Technology, Nanjing* 211101

(Received March 24, 2014; in final form June 9, 2014)

ABSTRACT

Tropical intraseasonal oscillation (including the Madden–Julian oscillation) is an important element of the atmospheric circulation system. The activities and anomalies of tropical intraseasonal oscillations affect weather and climate both inside and outside the tropical region. The study of these phenomena therefore represents one of the frontiers of atmospheric sciences. This review aims to synthesize and summarize studies of intraseasonal oscillation (ISO) by Chinese scientists within the last 5–10 years. We focus particularly on ISO's mechanisms, its numerical simulations (especially the impacts of diabatic heating profiles), relationships and interactions with ENSO (especially over the western Pacific), impacts on tropical cyclone genesis and tracks over the northwestern Pacific, and influences on the onset and activity of the South and East Asian monsoons (especially rainfall over China). Among these, focuses of ongoing research and unresolved issues related to ISO are also discussed.

Key words: tropical intraseasonal oscillation, Madden–Julian oscillation, mechanism, numerical simulation, ENSO

Citation: Li Chongyin, Ling Jian, Song Jie, et al., 2014: Research progress in China on the tropical atmospheric intraseasonal oscillation. *J. Meteor. Res.*, **28**(5), 671–692, doi: 10.1007/s13351-014-4015-5.

1. Introduction

Intraseasonal oscillation (ISO) is a dominant pattern of variability in the tropical atmosphere, with a period of approximately 40 days. ISO was firstly discovered in the 1970s by Madden and Julian (1971, 1972). Subsequent studies have found that ISO exists in the extratropics as well as in the tropics. The dominant component of tropical ISO, which propagates eastward, is the Madden–Julian oscillation (MJO). Intensive research on ISO (especially MJO) since the 1980s has revealed elements of the structure and activity of the MJO (Krishinamurti and Subrahmanyam, 1982; Murakami et al., 1984; Lau and Chan, 1985; Li, 1991; Madden and Julian, 1994; Zhang, 2005).

ISO impacts the onset and activity of the Asian summer monsoon (Mu and Li, 2000; Li et al., 2001; Lin et al., 2005) and summertime rainfall over China (Yang and Li, 2003; He et al., 2006; Zhang et al., 2009). The MJO also influences precipitation over many other regions, such as East Asia (Jeong et al., 2008), Southwest Asia (Barlow et al., 2005), Australia (Wheeler et al., 2008), and North America (Jones, 2000; Bond and Vecchi, 2003). These nonlocal influences are communicated through the circulation and teleconnections induced by anomalous convection associated with ISO in the tropics. The MJO can also modulate tropical cyclone (TC) genesis in northwestern Pacific, northern Indian Ocean, and the areas surrounding Australia. The active phase of the MJO in these regions sets a favorable state for TC genesis (Sobel and Maloney, 2000; Hall et al., 2001). Maloney

Supported by the National (Key) Basic Research and Development (973) Program of China (2010CB950400 and 2013CB956200).
*Corresponding author: lingjian@lasg.iap.ac.cn.

and Hartmann (2000a, b) showed that the frequency of TC genesis in the western Pacific increases when the active phase of MJO is also located in the western Pacific; however, other studies have suggested that the role of the MJO might not be the most important in modulating TC genesis (Liebmann et al., 1994). The details of how and why the MJO modulates TC genesis have yet to be clearly revealed.

Although the timescales of tropical ISO differ from that of ENSO, several studies have indicated significant interactions between these two phenomena. Li (1989) proposed that eastward propagating westerly anomalies in the tropical western Pacific associated with the MJO may play a pivotal role in the onset of El Niño. Many subsequent studies have confirmed the interactions between ISO in the tropical western Pacific (including the MJO) and ENSO, and have further shown that interannual variability in the intensity of ISO may also influence ENSO variability (Li, 1990; Li and Zhou, 1994; Li and Liao, 1998; Zhang and Gottschalck, 2002).

Numerical studies of ISO using atmospheric general circulation models (AGCMs) have drawn widespread attention in recent years. Total errors in numerical forecasts are significantly related to the ability of the forecast model to accurately predict the MJO (Hendon et al., 2000). These errors arise in large part from biases in the amplitude (weaker than observed) and eastward propagation (faster than observed) of the simulated MJO (Jones et al., 2000). Slingo et al. (1996) evaluated the ability of 15 AGCMs participating in the Atmospheric Model Intercomparison Project (AMIP) to simulate the MJO. They found that, although most models could capture ISO signals on intraseasonal timescales, none could reproduce the basic features of the observed MJO (such as the eastward propagation speed of 5–9 m s^{-1} or the seasonal cycle of MJO activity). Numerical studies of the MJO have been conducted by using a wide variety of models (Slingo and Madden, 1991; Maloney and Hartmann, 2001; Sperber, 2004; Kim et al., 2009), but the reasons that models are unable to accurately simulate the MJO remain unknown.

Chinese scientists have conducted a number of studies on ISO and the MJO in recent years, with significant progress on several fundamental issues. Some of these studies have focused on the impacts of the MJO on the spatiotemporal distribution of precipitation over China (Wu et al., 2009; Zhang et al., 2009; Bai et al., 2011; Jia and Liang, 2011; Jia et al., 2011; Zhang et al., 2011; Lü et al., 2012; Lin et al., 2013). Others have focused on how and why ISO influence TC activity in the northwestern Pacific (Zhu et al., 2004; Chen and Huang, 2009; Sun et al., 2009; Pan et al., 2010; Tian et al., 2010a, b; Zhu et al., 2013). Recently, some promising results of ISO have been used in the extended-range weather forecast, and positive results are obtained (Liang and Ding, 2012; Sun et al., 2013). Numerical studies have shown that the ability of a model to simulate the MJO depends not only on the ability of the model to simulate the large-scale atmospheric circulation and climate, but also on the method used to represent cumulus convection. Numerous studies have revealed the important role of diabatic heating in the lower level of the atmosphere for simulations of the MJO (Dong and Li, 2007; Jia and Li, 2007a, b; Li et al., 2007; Jia et al., 2008, 2009; Li et al., 2009; Ling et al., 2009; Jia et al., 2010; Yang et al., 2012). Important results have also been obtained regarding the interactions between the MJO and ENSO. Here, we provide a general review and discussion about studies of ISO and MJO conducted by Chinese scientists over the past decade.

2. Mechanisms of ISO/MJO

The mechanisms of ISO/MJO have been studied intensively since these phenomena were first identified; however, no existing hypothesis has been accepted as able to explain all of the observed features of ISO. Some early studies suggested that ISO was related to gravity waves in the tropical atmosphere (Chang, 1977), while others suggested that ISO might be induced by symmetric and asymmetric instability near the equator (Dunkerton, 1983). However, none of these hypotheses could explain the observed structure and eastward propagation of the MJO.

Li (1985) introduced the cumulus convective heating feedback mechanism (i.e., conditional instability of the second kind, or CISK), and showed that it could play an important role in the initiation and maintenance of MJO events in the tropics. Lau and Peng (1987) developed a mobile wave CISK theory that could better explain the slow eastward propagation of the MJO. Wang (1988) developed a frictional wave CISK theory and showed that the speed of the eastward propagating mode induced by deep convective latent heating triggered by low-level moisture convergence was similar to the observed propagation speed of the MJO. Li (1993) identified the potential for a dispersion CISK–Rossby wave to generate in the tropical atmosphere. This type of disturbance can propagate either westward or eastward when the CISK mechanism is introduced, and may be crucial for initiating and driving 30–60-day oscillations in the extratropical atmosphere.

Neelin et al. (1987) proposed an evaporation wind feedback mechanism, but subsequent studies indicated that this mechanism alone could not explain the initiation of the MJO. However, the evaporation wind feedback mechanism could induce unstable waves in the tropics, and may explain the characteristics of the MJO when combined with the CISK mechanism (Li, 1996). Li et al. (2002) studied MJO mechanisms using an air-sea coupled model that included both the CISK and evaporation wind feedback mechanisms, and found that the CISK mechanism played a more critical role in the dynamics of the simulated MJO. Air-sea coupling can reduce the frequency of the tropical waves induced by atmospheric disturbances, and could therefore play an important role in MJO dynamics.

Many numerical studies have confirmed the importance of lower tropospheric diabatic heating for simulating the MJO. We discuss results of these studies in detail later. Latent heating released during the formation of stratus clouds in the lower troposphere can also influence simulations of the MJO (Cha and Luo, 2011). Future studies of MJO mechanisms should pay particular attention to the distribution of diabatic heating in the middle and lower troposphere.

Zhang and Ling (2012) explored the dynamical structure and evolution of the MJO in terms of potential vorticity (PV). The structure of the MJO is an equatorial quadrupole of cyclonic and anticyclonic PV that tilts westward and poleward. This PV quadrupole is closely related to the swallowtail pattern of positive and negative precipitation anomalies associated with the MJO. Two processes dominate PV generation in the MJO. The first process is linear, and involves only MJO diabatic heating. The second is nonlinear, and involves diabatic heating and relative vorticity perturbations outside the MJO domain. These results highlight that the MJO has characteristics of both self-sustenance (linearity) and multiple-scale interactions (nonlinearity). The swallowtail precipitation pattern and the distribution of PV play important roles in the generation of the MJO.

Ling et al. (2014a) studied MJO events during the winter of 2006/2007 and identified large-scale patterns of PV and precipitation that favored MJO initiation. These patterns included a basin-scale (in the zonal direction) positive precipitation anomaly over the Indian Ocean and a persistent vertical dipole of PV generation (cyclonic PV generation in the lower troposphere and anticyclonic PV generation in the upper troposphere). Ling et al. (2013b) identified three large-scale patterns that precede MJO initiation over the Indian Ocean: low-level easterly anomalies that move from the western to the eastern Indian Ocean, zonal wavenumber-1 surface pressure anomalies with an equatorial low-pressure surge penetrating eastward from Africa through the Indian Ocean to the Maritime Continent, and eastward-moving negative temperature anomalies in the middle to upper troposphere over the Indian Ocean. All three of these patterns emerge approximately 20 days before convective initiation of the MJO and propagate eastward at speeds close to the typical propagation speed of the MJO (without any direct connection to MJO convection). These large-scale signals will be helpful for predicting the onset of MJO events.

3. Numerical simulation of ISO

Numerical simulation of ISO has been a hot topic in studies of ISO over the past several decades. Many AGCMs fail to reproduce the most salient features of the MJO, particularly its slow eastward propagation speed (Slingo et al., 1996; Kim et al., 2009). Errors related to the simulation of the MJO in numerical forecasts contribute substantially to total errors (Hendon et al., 2000). Typical errors in simulations of the MJO include an amplitude that is weaker than observed, an eastward propagation speed that is faster than observed, and an inability of the simulated MJO to propagate through the Maritime Continent (Jones et al., 2000). Improved numerical simulations of the MJO could substantially improve the accuracy of weather forecasts.

A number of factors can affect the ability of a numerical model to simulate the MJO. These factors often differ among different models. Some studies have shown that increasing horizontal resolution can improve simulations of the MJO (Hayashi and Golder, 1986), while other studies have shown little improvement with enhanced resolution (Duffy et al., 2003). Li and Yu (2001) found that introducing air-sea interactions substantially improved the simulated MJO, while other studies found no significant improvement. A variety of studies have suggested that the ability of a model to simulate the MJO depends critically on the convective parameterization employed in the model (Slingo et al., 1996; Wang and Schlesinger, 1999; Maloney and Hartmann, 2001). Jia et al. (2009) confirmed this result by using a variety of different cumulus parameterizations in the SAMIL (Spectral Atmosphere Model of State Key Laboratory of Numerical Modeling for Atmospheric Sciences and Geophysical Fluid Dynamics, Institute of Atmospheric Physics) AGCM. The ability of the model to simulate the MJO changed substantially when different cumulus parameterization schemes were used.

3.1 Impacts of the vertical distribution of diabatic heating

Li (1983) suggested that the vertical structure of latent heating due to condensation substantially influences the structure of the atmospheric circulation. Li et al. (2009) studied the impacts of the vertical structure of diabatic heating on the simulation of the MJO in SAMIL-R42L9. This model includes three optional cumulus parameterization schemes: the Tiedtke (TK) scheme (Tiedtke, 1989), the moisture convection adjustment (MCA) scheme (Manabe and Strickler, 1964), and the Zhang-McFarlane (ZM) scheme (Zhang and McFarlane, 1995). Figure 1 shows the zonal propagation of MJO zonal wind anomalies at 850 hPa simulated by SAMIL-R42L9 using the MCA and TK schemes. The model simulates the eastward propagation of the MJO well when the MCA scheme is used, but fails to simulate this feature when the TK scheme is used. These two model configurations generate substantially different vertical profiles of diabatic

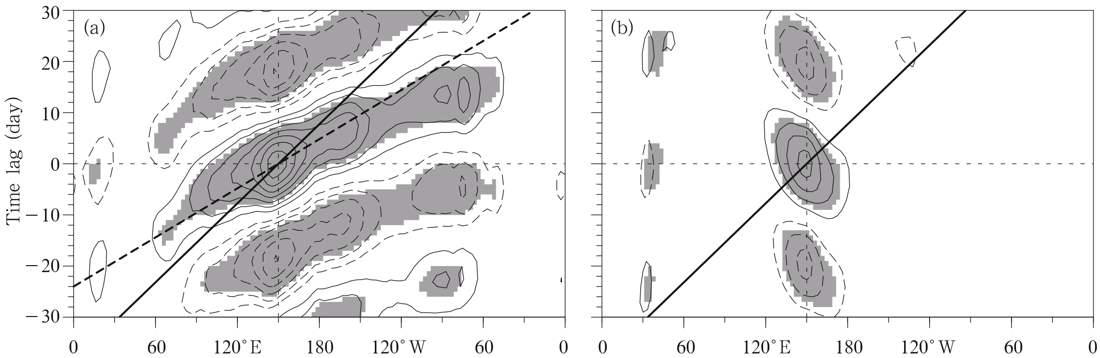

Fig. 1. Lag regression of MJO band-filtered (time periods of 30–90 days and zonal wavenumbers 1–5) zonal wind at 850 hPa (contour interval 0.2 m s^{-1}) averaged over 15°S–15°N on the reference point at 150°E. Data are from SAMIL simulations using (a) the MCA convection scheme and (b) the Tiedtke convection scheme. Dashed contours indicate negative values and zero contours are omitted. Shadings indicate significance at the 90% confidence level or above. Bold solid lines indicate eastward propagation at a speed of 5 m s^{-1}. [From Ling et al., 2013a]

heating. Diabatic heating peaks in the lower troposphere when the MCA scheme is used, but no such a peak exists when the TK scheme is used (figure omitted). These results suggest that the ability of this model to simulate the MJO depends critically on the vertical structure of diabatic heating in the model atmosphere.

Besides the control (CT) experiment, two additional numerical experiments were conducted by using SAMIL-R42L9 with the MCA scheme to further illustrate the impacts of different diabatic heating profiles on the simulated MJO. In one experiment, the latent heating profiles were modified at each time step and each grid to be "top heavy" (TH) in the tropical region (20°S–20°N). In the other experiment, the latent heating profiles were modified to be "bottom heavy" (BH), with a peak within 500–600 hPa. The vertically integrated diabatic heating remained unchanged when vertical distribution of diabatic heating profiles was modified in these two experiments. The tropical mean profiles of total diabatic heating in the CT and BH experiments are largely similar (although one was unmodified and the other was modified to increase latent heating at lower levels and decrease latent heating at upper levels). The tropical mean profile of total diabatic heating in the TH experiment is clearly top heavy, with a smaller amplitude.

Figure 2 shows the time evolution of intraseasonal diabatic heating profiles from these three simulations along with their associated zonal and vertical circulations. The diabatic heating anomaly and its associated circulation propagate eastward in the CT simulation at a phase speed of approximately 5.5 m s^{-1} (period of about 40 days). The circulation is characterized by a deep baroclinic mode that extends upward to 150 hPa, with mid-level upward motion, low-level convergence, and upper-level divergence in the region of heating. This manifestation of the MJO is completely absent in the TH simulation. The heating and cooling are weaker with a smaller zonal scale than in CT. Furthermore, no eastward propagation is apparent in either diabatic heating or the circulation. Evidently, the TH simulation does not produce the MJO. The results from the BH simulation are very similar to those from CT. Even though the tropical latent heating profiles were modified to be bottom heavy in BH, diabatic heating still penetrates upward into the upper troposphere. The eastward propagation speed of the MJO is slower (and closer to the observed propagation speed) in BH than in CT.

The results of these numerical experiments support the hypothesis proposed by Li (1983). The model reproduces the eastward propagation of the MJO when the vertical profile of diabatic heating peaks in the lower troposphere. Heating at lower levels induces strong upward motion and low-level moisture convergence, and sets favorable conditions for the generation and maintenance of deep convection. Furthermore, lowering the peak of the diabatic heating profile leads to slower eastward propagation in the simulated MJO. It is difficult to induce strong upward motion and low-level moisture convergence when the diabatic heating profile peaks in the upper troposphere. These conditions impede the development and maintenance of deep convection, and eliminate the MJO from the model simulation.

3.2 Impacts of latent heating in the boundary layer

Figure 1 shows that the SAMIL-R42L9 cannot accurately simulate the MJO when the TK scheme is used. This inability to simulate the MJO arises from the parameterization itself. Ling et al. (2013a) showed that the vertical distribution of diabatic heating above the planetary boundary layer (PBL) in SAMIL is similar regardless of whether the MCA or TK scheme is used. The main differences in diabatic heating are located within the PBL. The TK scheme produces a significant peak in latent heating in the PBL that does not appear when the MCA scheme is used. This distinct peak in latent heating in the PBL also appears in global reanalysis data and in other AGCMs, such as the Community Atmosphere Model version 3 (CAM3) and the Tropical channel Weather Research and Forecasting (TWRF) model. These models are also unable to simulate the eastward propagation of the MJO. Distributions of latent heating in two recent global reanalysis datasets, the Climate Forecast System Reanalysis

(CFSR; Saha et al., 2010) and the Modern Era Retrospective Analysis for Research and Applications (MERRA; Bosilovich et al., 2006), have obvious peaks in the PBL (Ling and Zhang, 2011). Free runs of the

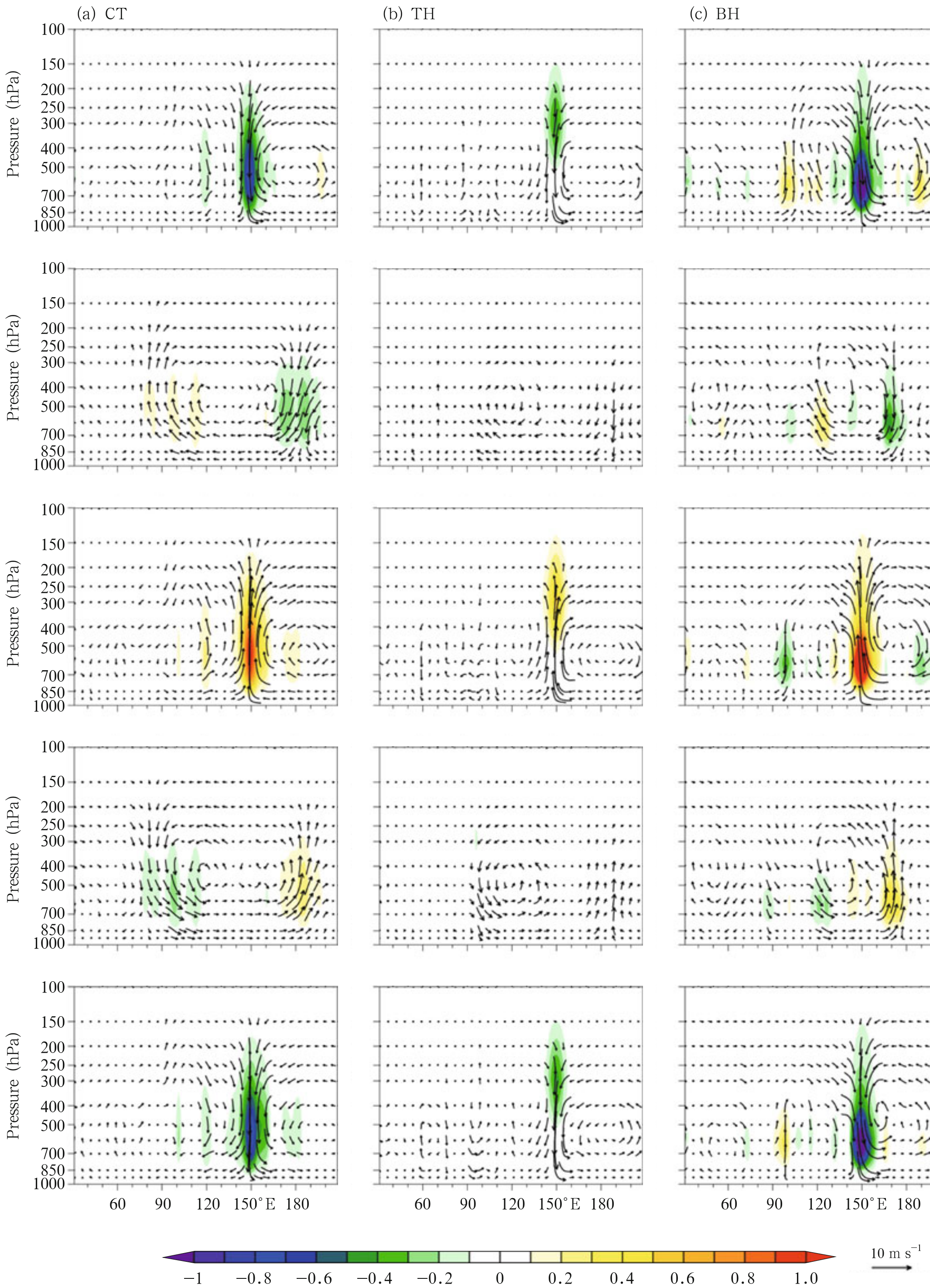

Fig. 2. Lag regression of intraseasonal (30–60-day) diabatic heating (color shading; K day^{-1}) and zonal-vertical wind vectors averaged over the tropics (15°S–15°N) on vertically integrated heating at 150°E based on the CT (left), TH (middle), and BH (right) experiments. [From Li et al., 2009]

atmospheric models used in these two reanalysis datasets have been unable to reproduce the characteristics of the MJO well (see results based on CFS and GEOS5 presented by Kim et al., 2009). The peak in latent heating in the PBL may be the reason that SAMIL is unable to simulate the eastward propagation of MJO when the TK scheme is used. Numerical experiments conducted using a version of SAMIL with increased vertical resolution (SAMIL-R42L26) help to improve the description of convection in the vertical direction.

The Tiedtke scheme is a mass flux convection scheme that can represent shallow, deep, and mid-level convective events (Tiedtke, 1989; Nordeng, 1994). The impacts of the latent heating peak in the PBL on the simulation of the MJO are explored by using another set of sensitivity simulations. In one simulation, latent heating generated by shallow convection was set to zero at each time step; this simulation is referred to as the no-shallow-latent-heating (NSLH) run. Latent heating due to shallow convection was doubled relative to the control simulation in the second sensitivity simulation; this simulation is referred to as the double-shallow-latent-heating (DSLH) run. Total latent heating therefore does not match precipitation in the NSLH or DSLH runs at grid locations where shallow convection occurs. The effects of this mismatch between precipitation and latent heating are relatively minor because the water vapor source over the ocean (where most shallow convection occurs in this model) does not depend on precipitation. The equivalent precipitation (EPR) derived from latent heating is used as the regression index in place of precipitation. EPR is linearly related to vertically integrated latent heating. Figure 3 shows the propagation of band-pass filtered 850-hPa zonal wind and EPR anomalies averaged over the tropics (15°S–15°N) for each of the three experiments. Neither 850-hPa zonal wind anomalies nor EPR anomalies propagate eastward in the control or DSLH runs (in fact, these anomalies show signs of weak westward propogation). By contrast, anomalies in 850-hPa zonal wind and EPR both propagate eastward from the Indian Ocean to the western Pacific Ocean in the NSLH run. The propagation speed for these anomalies is similar to (though slightly faster than) the observed propagation speed of the MJO. These results show that SAMIL using the TK scheme can simulate the eastward propagation of the MJO when latent heating from shallow convection is removed.

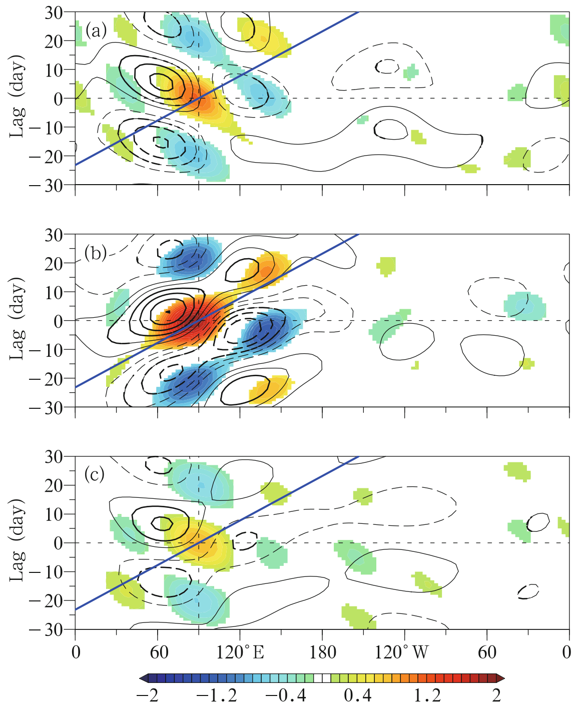

Fig. 3. Lag regression of MJO band-filtered 850-hPa zonal wind (U850; contours; interval 0.2 m s^{-1}) and EPR (color shading; mm day^{-1}) upon EPR at 90°E (day 0) from (a) the control run, (b) the no-shallow-latent-heating (NSLH) run, and (c) the double-shallow-latent-heating (DSLH) run. All data are averaged over 15°S–15°N. Dashed contours indicate negative values and zero contours are omitted. Only results passing a significance test at the 90% confidence level or above are shown for EPR. Significance at the same level is shown by thick contours for U850. The thick blue solid lines indicate eastward propagation at a speed of 5 m s^{-1}. [From Ling et al., 2013a]

Figure 4 shows the distributions of latent heating and large-scale horizontal moisture convergence in the control and NSLH runs together with their associated zonal and vertical circulations. Low-level moisture convergence is weak, shallow, and small (on zonal scale) in the control run. By contrast, low-level moisture convergence is stronger and deeper in the NSLH

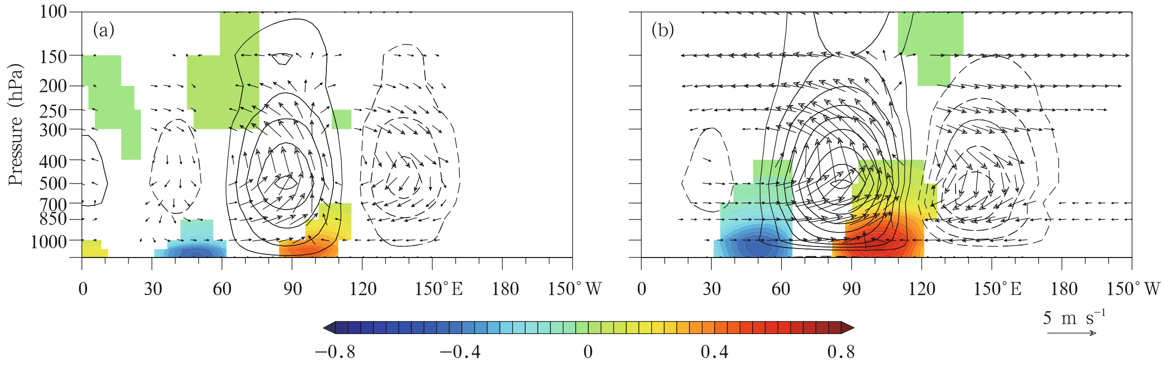

Fig. 4. Longitude-pressure distributions of tropical (15°S–15°N) mean latent heating (contours; interval 0.1 K day^{-1}), moisture convergence (color shading; 10^{-5} g kg^{-1} s^{-1}), and zonal-vertical wind vectors regressed on MJO EPR at 90°E with a 0-day time lag based on (a) the control run and (b) the no-shallow-latent-heating (NSLH) run. Dashed contours indicate negative values and zero contours are omitted. Only results passing a significance test at the 90% confidence level or above are plotted for moisture convergence and zonal-vertical wind. Significance at the same level is indicated by thick contours for latent heating. [From Ling et al., 2013a]

run, with a broader zonal scale. The NSLH run includes a strong center of low-level moisture convergence extending up to 500 hPa located east of the latent heating center. This center of low-level moisture convergence supplies moisture to and establishes favorable conditions for the generation of deep convection over the region east of the existing convection. This result is consistent with the role of boundary layer frictional convergence in MJO theory (Wang, 1988), and may explain the eastward propagation of the simulated MJO in the NSLH run. The differences in low-level moisture convergences between these two sensitivity simulations are related to shallow convection simulated by the Tiedtke scheme, which generates a peak in latent heating in the PBL. This peak tends to confine moisture to the PBL and limit moisture transport into the free atmosphere, leading to a dry bias in the free atmosphere that effectively eliminates MJO variability from the simulation.

3.3 Impacts of cumulus momentum transport

Cumulus convection is the most important physical process in the tropical atmosphere. In addition to the release of latent heating due to condensation in cumulus convection, vertical momentum transport in convection substantially influences the tropical atmospheric circulation.

Li (1984) showed that vertical cumulus momentum transport could act as a kind of Ekman pumping that influences the formation and maintenance of typhoons, as well as the development of the ITCZ. Modeling studies show that the mean state of the atmospheric circulation can be improved by introducing convective momentum transport (Zhang and McFarlane, 1995; Gregory et al., 1997; Inness and Gregory, 1997). In particular, convective momentum transport suppresses the development of deep convection (Tung and Yanai, 2002) and reduces precipitation (Wu et al., 2007) in the tropics. Relatively few studies have focused on the impacts of vertical cumulus momentum transport on the simulation of the MJO. Ling et al. (2009) conducted several numerical experiments using the CAM2 AGCM with the Tiedtke scheme, and found that, although the general circulation in the model is improved when vertical momentum transport is introduced, the ability of the model to simulate the MJO deteriorates.

None of the model simulations presented in Section 3.2 contain vertical cumulus momentum transport, and yet the simulated MJO is substantially different between the control and NSLH simulations. Ling and Li (2014) introduced vertical cumulus momentum transport to these two experiments (referred to as CTCMT and NSCMT, respectively).

The strength of the simulated MJO is weakened when vertical cumulus momentum transport is introduced. In particular, the zonal propagation of EPR and 850-hPa zonal wind anomalies are dramatically different between the NSCMT and NSLH runs. The amplitudes of these anomalies are reduced, and the eastward propagating signals over the western Pacific disappear. The diabatic heating profiles in the control experiment do not change significantly when vertical cumulus momentum transport is included; however, the diabatic heating profiles in the NSLH experiment change dramatically when vertical cumulus momentum transport is included. The reason for this difference is that deep convection is not simulated well in the control experiment, so the impact of vertical momentum transport by deep convection is not adequately represented. This difference is also reflected in the simulations of precipitation. Changes in tropical precipitation following the addition of vertical momentum transport are much larger in the NSLH experiment than in the control experiment (figure omitted).

These results show that the ability of a model to simulate the MJO can be significantly affected by the inclusion (or exclusion) of vertical cumulus momentum transport, even for models that simulate the MJO well. The influence of vertical cumulus momentum transport on the simulation of the MJO also appears to depend on the ability of the original model to simulate the MJO (especially its eastward propagation).

4. Relationship between the MJO and ENSO

The MJO and ENSO are two modes of climate variability that operate on different timescales. A large number of studies have examined the relationships between these two modes of climate variability. Li (1989) suggested that a strong East Asian winter monsoon could help to initiate an El Niño event by exciting a strong MJO over the equatorial western Pacific. Many subsequent studies have shown evidence of interactions between the MJO over the equatorial western Pacific and ENSO (Li, 1990; Li and Zhou, 1994; Long and Li, 2002; Zhang and Gottschalck, 2002). The influence of the MJO on ENSO is largely attributable to interannual variability in the intensity of MJO activity (Li and Liao, 1998; Li et al., 2003, 2008).

Numerous studies have shown strong relationships between the intensity of MJO activity over the equatorial western Pacific and the occurrence of ENSO. MJO activity over the equatorial western Pacific is generally stronger before the occurrence of El Niño, and then weakens rapidly as El Niño develops. A strong MJO is associated with strong westerly wind anomalies over the equatorial western Pacific, which induce anomalous oceanic Kelvin waves that can trigger El Niño. The standard deviation of low frequency (30–60 days) kinetic energy is largest (> 0.9) over the equatorial western Pacific (figure omitted), which indicates that MJO activity over the equatorial western Pacific plays an important role in the interannual variation of low frequency oscillations in the tropical atmosphere. Figure 5 shows the composite evolution of sea surface temperature anomalies (SSTA) in the Niño 3.4 region and low frequency (30–60 days) kinetic energy anomalies at 850 hPa over the equatorial western Pacific (10°S–10°N, 130°E–180°) based on five strong El Niño events. The SSTA in the Niño 3.4 region shows the life cycle of El Niño. The MJO-related kinetic energy anomalies over the equatorial western Pacific are positive during the spring and summer preceding the mature phase of El Niño, but decrease significantly when El Niño reaches its mature phase. These results suggest a significant relationship between the interan-

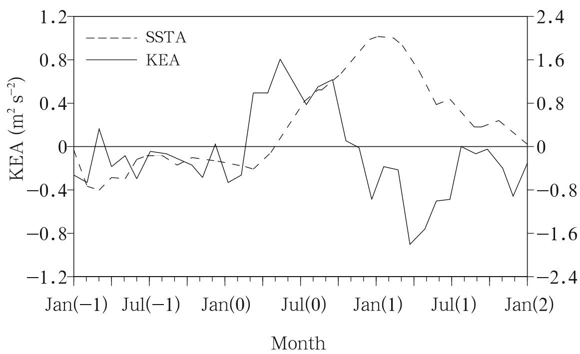

Fig. 5. Composite evolution of SSTA (dashed line; ℃) in the Niño 3.4 region and kinetic energy anomalies associated with the atmospheric intraseasonal oscillation (KEA; solid line; $m^2\ s^{-2}$) over the equatorial western Pacific over five strong El Niño events. The axis label 0 indicates the year of El Niño onset. [From Li et al., 2008]

nual variability of MJO activity over the equatorial western Pacific and El Niño. A strong positive anomaly in MJO activity over the equatorial western Pacific favors the development of an El Niño event; conversely, the development of an El Niño event inhibits MJO activity.

A number of studies during the early 21st century have focused on characterizing the relationships between ENSO and the MJO. Several studies abroad show clear relationships between MJO variability and ENSO variability (Roundy and Kriavitz, 2009; Gushchina and Dewitte, 2012), and support the idea that the intensification of MJO activity over the equatorial western Pacific during boreal spring favors the development of El Niño (Hendon et al., 2007; Marshall et al., 2009). Some studies suggested that the relationships between the MJO and ENSO are due to the response of the ocean to MJO activity (Zavala-Garay and Zhang, 2004; Zavala-Garay et al., 2008; Seiki et al., 2009), which is inherently nonlinear (Tang and Yu, 2008). The influence of the MJO on ENSO has also been investigated by using the delayed oscillator model (Richard et al., 2008). Analyses of observations and numerical simulations indicate that the influence of MJO activity on ENSO can be treated as a stochastic forcing (Kapur et al., 2011).

Chinese scientists made several promising advances toward understanding the relationships between the MJO and ENSO over the past several years. Liu et al. (2008) used an intermediate air-sea coupled model to study the influence of the MJO on ENSO. Their experiments involved forcing the ocean component with MJO zonal wind anomalies of different amplitudes. Several major features of ENSO are successfully simulated in the control run, such as the typical 4-yr period of oscillations in SSTA in the Niño 3 region (5°S–5°N, 90°–150°W), the tendency of ENSO events to occur predominantly between September and December, and the 2–7-yr interval between successive ENSO events. The results of these simulations suggest that weak MJO signals can intensify the amplitude of ENSO, while very strong MJO signals decrease the amplitude of ENSO. The typical period of ENSO variability in the model is unaffected by the existence of the MJO forcing. Peng et al. (2011) suggested that stochastic forcing associated with the MJO affects the predictability of ENSO. Rong et al. (2011) showed that high frequency ($<$ 90 days) variability in near-surface winds impacts the development of SSTA associated with ENSO. Most high frequency variability in near-surface wind in the equatorial western Pacific is related to MJO activity, so these impacts can be regarded as indicative of the relationship between MJO activity and ENSO.

El Niño events can be classified into three categories: Eastern Pacific (EP) El Niño, Central Pacific (CP) El Niño, and mixed-type El Niño (Yuan, 2009). MJO kinetic energy over the western Pacific may influence the evolution of these different types of El Niño in different ways. Figure 6 shows time-latitude cross-sections of MJO kinetic energy at 850 hPa and its anomaly averaged over the western Pacific region (120°–160°E) associated with the three types of El Niño. EP El Niño (Fig. 6a) is associated with strong MJO activity both in the Northern Hemisphere from the previous winter through the onset of El Niño and in the Southern Hemisphere between June and October before the onset of El Niño. The strength of MJO is reduced dramatically after the onset of EP El Niño. This negative anomaly can last through the following winter. CP El Niño (Fig. 6b) is associated with seasonal north-south migration in MJO anomalies before the onset of El Niño. Anomalies in MJO kinetic energy are strong and positive in the Southern Hemisphere during the preceding boreal winter and in the Northern Hemisphere during the preceding boreal spring and summer. The onset of CP El Niño leads to the emergence of negative anomalies in MJO kinetic energy near 10°N, but enhances the positive anomalies in the Southern Hemisphere. Mixed-type El Niño (Fig. 6c) is associated with enhanced MJO activity in both the Southern and Northern Hemispheres during the period May–August preceding the El Niño. Anomalies in MJO kinetic energy are positive near 10°S but negative in the Northern Hemisphere following the onset of El Niño. MJO activity is anomalously strong over the equatorial western Pacific before the onset of each type of El Niño, despite some differences in the

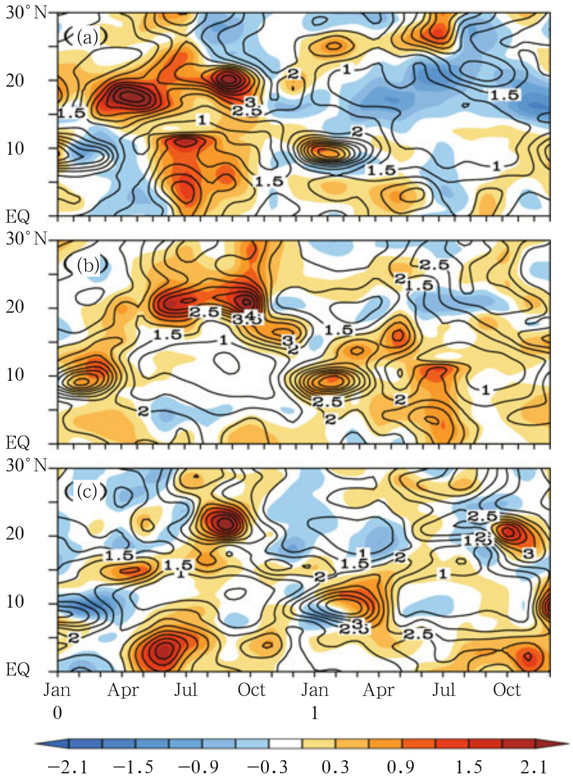

Fig. 6. Time-latitude cross-sections of MJO kinetic energy at 850 hPa (contours; m^2 s^{-2}) and its anomaly (color shading; m^2 s^{-2}) in the western Pacific (120°–160°E) during (a) EP, (b) CP, and (c) mixed-type El Niños, respectively. The axis label 0 indicates the year of El Niño onset (1 indicates the following year).

detailed distribution.

MJO activity can also be described by using outgoing longwave radiation (OLR), which captures the strong convective activity associated with the MJO. The canonical dipole pattern of OLR anomalies associated with ENSO can be identified over the tropical Pacific Ocean for all three types of El Niño (figure omitted), but the distribution of OLR anomalies is somewhat different. The dipole is strongest in amplitude, largest in zonal scale, and longest in duration (nearly 1 yr) for EP El Niño; and weakest in amplitude, smallest in zonal scale, and shortest in duration (6 months) for CP El Niño. The positive and negative OLR anomalies are centered near 160°W and 130°E, respectively, during EP El Niño; and near 180° and 110°E, respectively, during CP El Niño. The entire dipole is shifted westward during CP El Niño relative to that during EP El Niño. The evolution of these OLR anomalies has some similarities for the three types of El Niño, along with several differences. The characteristics of this evolution indicate that MJO activity and El Niño development are closely related, and that MJO activity might be different under different types of El Niño.

5. Influences of ISO on weather and climate

5.1 ISO and TC genesis over the northwestern Pacific

5.1.1 Impacts of MJO on TC genesis over the northwestern Pacific

Pan et al. (2010) examined relationships between MJO variability and TC activity over the northwestern Pacific using the real-time multivariate MJO (RMM) index (Wheeler and Hendon, 2004) generated at the Centre for Australian Weather and Climate Research. The RMM index describes both the strength of the MJO and its spatial distribution (particularly the location of the active phase of MJO convection). The number of TCs generated over the western Pacific during typhoon season (June–October) are counted and classified according to different phases of the MJO between 1979 and 2004 based on the TC data compiled by the Joint Typhoon Warning Center (JTWC), the Shanghai Typhoon Institute, and the Japan Meteorological Agency (JMA). MJO variability has substantial impacts on TC genesis. The number of TCs generated during typhoon season under strong MJO events is almost twice the number of TCs generated under weak MJO events. The results are consistent regardless of the TC dataset used. This result indicates that TCs are more likely to form during strong MJO events. TC genesis also depends on the phase of the MJO. The total number of TCs generated during phases 5 and 6 (when the active convection center is located over the western Pacific; hereafter referred to as the Pacific phase), is much greater than the number of TCs generated during phases 2 and 3 (when the active convection center is located over the Indian Ocean; hereafter referred to as the Indian Ocean phase).

A number of factors contribute to the differences in the number of TCs generated during the Pacific and Indian Ocean phases of the MJO. Composite distributions of the large-scale circulation, sea surface pressure, ITCZ, vertical motion, and convective heating during the Pacific phase are substantially different from those during the Indian Ocean phase. The Indian Ocean phase of the MJO is characterized by positive anomalies of sea surface pressure, large vertical wind shear, negative anomalies in convective heating, and weak vertical motion over the northwestern Pacific. All of these conditions inhibit the genesis and development of TCs over the northwestern Pacific. By contrast, the Pacific phase of the MJO is characterized by negative anomalies of sea surface pressure, small vertical wind shear, positive anomalies in convective heating, and strong vertical motion over the northwestern Pacific. These conditions all favor TC genesis over the northwestern Pacific. The large-scale dynamical environment over the northwestern Pacific, which plays an important role in TC genesis, changes significantly as the MJO propagates eastward from the tropical Indian Ocean.

5.1.2 Impacts of ISO on TC genesis over the northwestern Pacific

Tian et al. (2010b) further studied the impacts of ISO on TC genesis in the northwestern Pacific by comparing the differences between composites of low-frequency kinetic energy at 850 hPa for years with larger and smaller numbers of TCs. Positive anomalies in low-frequency kinetic energy are observed over the northwestern Pacific east of the Philippines and south of 15°N (an area typically dominated by the monsoon trough) during the years with large numbers of TCs. This relationship indicates that strong low-frequency activity can enhance the monsoon trough and promote TC genesis. By contrast, the years with less TC genesis are characterized by positive anomalies in low-frequency kinetic energy over the Indian Peninsula and the southern part of the South China Sea and negative anomalies over the area east of the Philippines.

The amplitude of ISO can also be quantified in terms of the 30–60-day bandpass-filtered zonal wind at 850 hPa. ISO activity is considerably different during years with more TC genesis than during years with less TC genesis. In particular, ISO activity in the monsoon trough region over the northwestern Pacific tends to be strong during years with more TC genesis and weak during years with less TC genesis.

A strong low-frequency cyclonic circulation extends eastward to 160°E over the western Pacific during years with more TC genesis, covering approximately the same area as the monsoon trough. This suggests that strong ISO activity intensifies the low-pressure system associated with the monsoon trough and extends it toward the east. Furthermore, the low-frequency velocity potential at 200 hPa indicates significant divergence over the northwestern Pacific to the east of the Philippines during years with more TC genesis. Both of these conditions are favorable for TC genesis in the northwestern Pacific.

5.2 ISO and TC tracks over the northwestern Pacific

Forecasts of TC tracks are an important part of predicting the activity and impacts of TCs. Previous studies have shown that the effects of ISO on the large-scale circulation (particularly the distribution and location of the monsoon trough and subtropical high) influence TC tracks in the northwestern Pacific (Harr and Elsberry, 1991; Carr and Elsberry, 1995; Hu et al., 2005). These relationships between ISO activity and TC tracks can be used to improve TC forecasts.

TC tracks in the northwestern Pacific can traditionally be classified into three categories: tracks that move directly westward, tracks that move northwestward, and tracks that recurve. Tian et al. (2010a) further divided the recurving tracks into three categories based on the direction of movement after the recurve: tracks that recurve to the west of Japan (i.e., those that approach the Korean Peninsula after recurving), tracks that make landfall over Japan, and tracks that recurve to the east of Japan. Tracks that move directly westward are the most common of these types during the typhoon season, followed by recurving TCs that make landfall over Japan and recurving TCs that pass to the east of Japan. The occurrence frequency of these different types of TC tracks also varies from month to month. The occurrence frequency of westward-moving typhoons is highest in July, while the occurrence frequencies of northwestward-moving TCs and recurving TCs that make landfall over Japan are highest in August. A full half of the northwestward-moving TCs occur in August, while no TCs of this type occur in June or October. Most of the TCs that recurve to the east of Japan occur in October.

Figure 7 shows composite low-frequency (ISO) horizontal wind fields at 850 hPa corresponding to the five different types of TC tracks (Tian et al., 2010a). These composites are constructed relative to the time of TC genesis over the northwestern Pacific. All five types of TC tracks occur under the influence of low-frequency cyclonic (LFC) anomalies over East Asia and the northwestern Pacific, but the location and pattern of the LFC anomaly are unique for each type. TCs that move directly toward the west (Fig. 7a) are associated with an anomalous LFC circulation over the South China Sea (SCS) and the Philippine Sea, with a low-frequency anticyclone (LFAC) anomaly located to its north. TC tracks that move directly toward the northwest (Fig. 7b) are associated with an anomalous LFC circulation over Taiwan Island, which extends eastward to 160°E. This circulation acts to intensify the monsoon trough and extends it toward the west, and is located southwest of an anomalous LFAC. The belt of the anomalous LFC (i.e., the region of

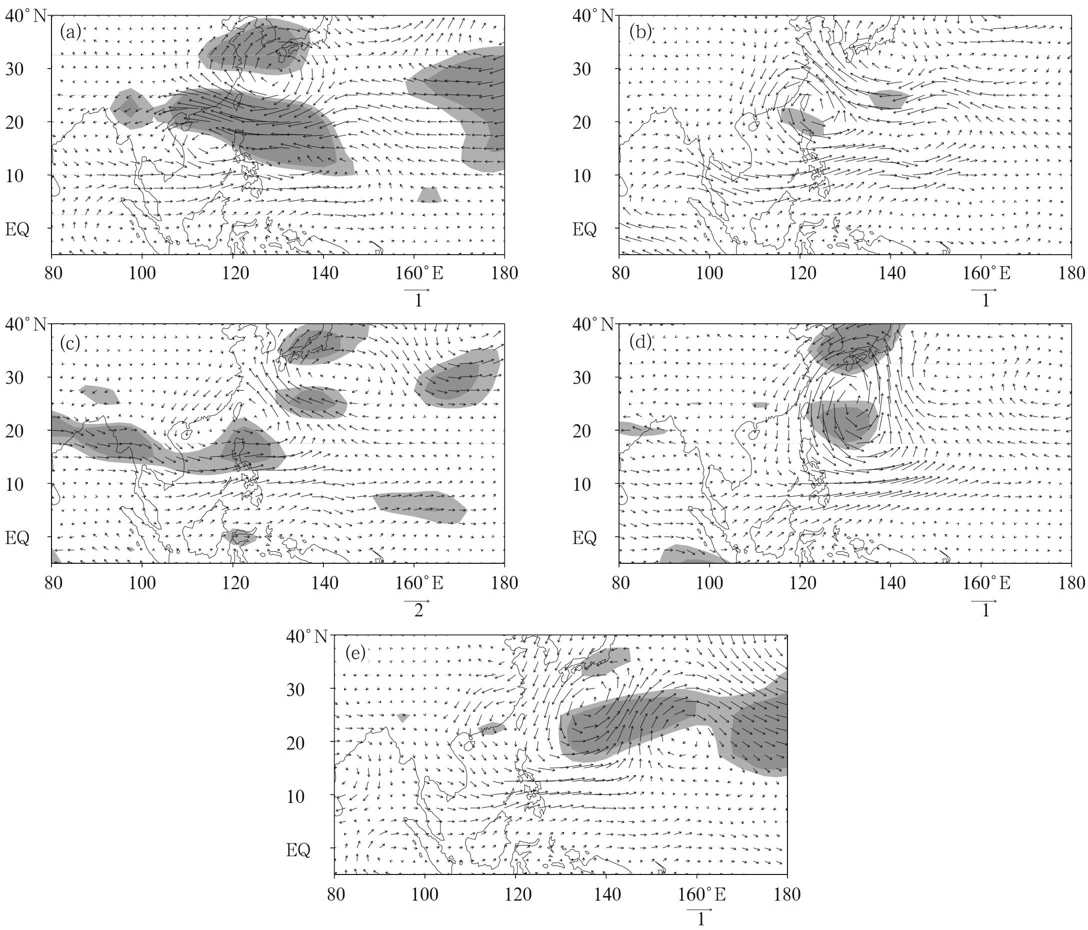

Fig. 7. Composites of 30–60-day bandpass-filtered wind vectors (m s^{-1}) at 850 hPa for different types of typhoon tracks: (a) typhoons that move directly westward, (b) typhoons that move northwestward, (c) typhoons that recurve to the west of Japan, (d) typhoons that make landfall over Japan, and (e) typhoons that recurve to the east of Japan. Light shadings indicate significance at the 95% confidence level, while dark shadings indicate significance at the 99% confidence level. [From Tian et al., 2010a]

maximum positive vorticity) extends zonally from the SCS to the Philippine Sea for westward-moving TCs, but tilts toward the northwest for northwestward-moving TCs. TCs tend to move along this belt of positive low-frequency vorticity.

TCs that recurve to the west of Japan (Fig. 7c) are associated with an anomalous LFC circulation over the East China Sea and Yellow Sea and a strong anomalous LFAC circulation near 30°N, 130°–160°E. TCs in this regime generally move northward over the belt of positive low-frequency vorticity west of 130°E and make landfall over the Korean Peninsula. Recurving TCs that make landfall over Japan (Fig. 7d) are associated with an anomalous LFC circulation that covers a large area between the Philippines and Japan (10°–35°N, 120°–145°E). TCs under this regime move northward over Japan following this belt of positive low-frequency vorticity. TCs that recurve to the east of Japan (Fig. 7e) are associated with an anomalous LFC circulation that slants northeastward from southern Japan and an anomalous LFAC circulation centered near 20°N, 150°–166°E. These TCs follow this belt of positive low-frequency vorticity northeastward over the ocean to the east of Japan. The pattern of the anomalous LFC circulation at 850 hPa (particularly the belt of positive low-frequency vorticity) plays a key role in determining TC tracks over the northwestern Pacific. This relationship between ISO and TC tracks can be used to improve predictions of TC tracks in the northwestern Pacific.

All five types of TC tracks are consistently associated with low-frequency westerly anomalies near the equator between the Indian Ocean and 150°E. This relationship further confirms the positive relationship between ISO activity in the tropical Pacific and TC genesis over the northwestern Pacific.

Analysis of composite low frequency wind fields at 200 hPa (figure omitted) further supports these results. TC tracks generally follow regions of strong horizontal winds located southwest of the upper tropospheric LFAC. The composite location and horizontal distribution of the upper tropospheric LFAC and the amplitude and direction of the maximum horizontal wind southwest of this LFAC differ for different types of TC tracks. These differences are then manifested in the direction of TC movement.

5.3 Impacts of ISO on the Asian summer monsoon

5.3.1 ISO and the onset of the Asian summer monsoon

Mu and Li (2000) studied the relationship of the onset of the South China Sea (SCS; 5°–20°N, 105°–120°E) summer monsoon and local ISO activity. The results have highlighted the important roles of the temporal evolution of 850-hPa zonal wind, the low-frequency (30–60 days) variability in zonal wind, and low-frequency variability in kinetic energy. Increases in the amplitude of low-frequency westerly winds over the SCS are primarily attributable to both westward extension of low-frequency westerly wind variability from the east and local excitement (figure omitted).

The onset of the SCS summer monsoon is preceded by the development of a symmetric pair of off-equatorial cyclones at 850 hPa over the tropical Indian Ocean (Zhou and Chan, 2005). The development of this symmetric pair of cyclones is dominated by 30–60-day low-frequency waves. These results suggest that the onset of the SCS summer monsoon is fundamentally related to ISO variability over the tropical Indian Ocean. The development of the symmetric cyclonic circulations leads the onset of the SCS summer monsoon by approximately 5–10 days. The emergence of the low-frequency cyclonic circulations over the tropical Indian Ocean can therefore be considered an indicator of the imminent onset of the SCS (or Asian) summer monsoon.

5.3.2 Impacts of ISO on the East Asian summer monsoon

Variability in the East Asian (EA) summer monsoon dramatically impacts the weather and climate of Asia, including the occurrence of floods and droughts in East China. Li et al. (2001) have identified years of strong (1981, 1984, 1985, 1986, 1990, 1992, and 1997) and weak (1980, 1983, 1987, 1989, 1991, 1993, and 1998) SCS/EA summer monsoons. The composite circulation anomalies for years with strong summer monsoons are distinctly different from the composite anomalies for years with weak summer monsoons. Years with strong summer monsoons are characterized by stronger westerly winds between 5° and 20°N and stronger easterly winds between 5° and 20°S. The cyclonic circulation located northeast of the SCS is also stronger during these years. ISO activity at 850 hPa is intense during strong monsoon years, particularly over the SCS and Philippines. ISO activity is much weaker (by about a factor of two) during years with weak summer monsoons. The most intense ISO activity during weak years is located over the northwestern Pacific (20°N, 140°E). The formation of a strong cyclonic circulation is one of the most important characteristics of a strong SCS summer monsoon. ISO activity and low-frequency cyclonic circulation anomalies over the SCS and adjacent regions play an important role in determining the strength of this cyclonic circulation and therefore the strength of the EA summer monsoon.

A powerful anticyclone develops in the upper troposphere (approximately 200 hPa) over the Tibetan Plateau during the Asian summer monsoon. This upper tropospheric anticyclone is observed during both strong and weak summer monsoons, but it is stronger and displaced toward the northwest during strong summer monsoons. Moreover, the most pronounced difference in ISO activity between strong and weak summer monsoons is located over the Tibetan Plateau (figure omitted). In particular, low-frequency anticyclonic circulation anomalies over the Tibetan Plateau are more intense during strong summer monsoons. This relationship indicates that ISO activity over the Tibetan Plateau (particularly, the low-frequency anticyclonic circulation anomalies) plays an important role in the onset and maintenance of strong EA summer monsoons.

5.3.3 Impacts of ISO on the Indian summer monsoon and precipitation over Yunnan Province, China

The Indian (South Asian) summer monsoon is an important component of the Asian summer monsoon system and has significant impacts on summer weather and climate throughout Asia, including China. The onset and variability of the South Asian summer monsoon are closely related to ISO activity (Murakami et al., 1986; Wang and Xu, 1997; Goswami and Mohan, 2001; Goswami et al., 2003). The evolution of prevailing westerlies in the lower troposphere (one of the distinguishing features of the Indian summer monsoon circulation) depends fundamentally on the nonlinear effects of ISO (Qi et al., 2009). Nonlinear momentum transport by ISO disturbances contributes approximately 40% of the momentum required to establish westerly winds over the Indian monsoon region in early June, and also contributes to the weakening of these westerly winds after mid July. Surface wind convergence and air-sea interactions associated with MJO convection in the western equatorial Indian Ocean propagate both eastward and northward, during the onset of the Indian summer monsoon (Qi et al., 2008).

Interannual variability in the Indian summer monsoon and interannual variability in local ISO activity are out of phase. Strong ISO activity is associated with anticyclonic anomalies in the lower troposphere over the Indian subcontinent, corresponding to a weak Indian summer monsoon (Qi et al., 2009). Conversely, weak ISO activity is associated with cyclonic anomalies that correspond to a strong Indian monsoon. A strong Indian summer monsoon also tends to suppress convection in the eastern equatorial Indian Ocean and weaken northward-propagating ISO, thus resulting in weak ISO activity in the Indian monsoon region (Qi et al., 2008). These results indicate substantial interactions between ISO and the Indian summer monsoon.

Lü et al. (2012) have shown that persistent MJO anomalies over the central and eastern tropical Indian Ocean can influence summer precipitation in Yunnan Province, China. A persistent positive phase of the MJO suppresses convective activity over the Bay of Bengal. This situation is associated with drought conditions in Yunnan Province. By contrast, a persistent negative phase of the MJO enhances convective activity over the Bay of Bengal and increases summer rainfall over most parts of Yunnan Province (except northwestern Yunnan and the eastern parts of central Yunnan). These results indicate that interannual variations in MJO activity over the tropical Indian Ocean have a significant impact on summer precipitation over Yunnan Province. A positive MJO induces subsidence over the tropical Indian Ocean region (70°–110°E). This may lead to a weaker monsoon vertical circulation over South Asia, decreasing moisture transport from the tropical Indian Ocean, and reducing precipitation over Yunnan Province.

5.4 The MJO and precipitation over China

Impacts of MJO variability on the spatiotemporal distribution of precipitation over China have been investigated extensively during recent years (Wu et al., 2009; Zhang et al., 2009; Bai et al., 2011; Jia and Liang, 2011; Jia et al., 2011; Zhang et al., 2011; Lü et al., 2012; Lin et al., 2013). The distribution and magnitude of precipitation over different parts of China vary significantly under different phases of the MJO.

The MJO is a cluster of strong convective events propagating eastward along the equator. In addition to tropical Rossby and Kelvin waves, this cluster of strong convective events induces an extratropical Rossby wave train that emanates from the tropics toward high latitudes. This extratropical Rossby wave train induces remote responses in precipitation. The spatial pattern of these responses is very different under different seasons and different phases of the MJO due to changes in the atmospheric background state and the location of the anomalous convective heating. Anomalous convective activity associated with the different phases of the MJO helps to establish favorable (or unfavorable) conditions for rainfall over various parts of China (especially East China), and is therefore an important factor in determining the distribution of anomalous precipitation over China.

6. Conclusions

ISO (including the MJO) is an important component of the climate system. ISO (and associated anomalies) exerts substantial influences on many aspects of weather and climate, so understanding the structures, characteristics, and dynamical mechanisms of ISO is prerequisite to understanding the climate system. Studies of ISO therefore represent one of the frontiers of atmospheric sciences. This study has briefly reviewed and summarized the main achievements of Chinese scientists in this field over the past decade. The main results are as follows.

The dynamical mechanisms of tropical ISO, and particularly the MJO, have been under investigation since the 1970s. Studies have suggested that feedbacks associated with heating due to cumulus convection are fundamental to the existence of the MJO. Recent numerical simulations support this idea, and reveal that the vertical distribution of diabatic heating in the tropics plays an important role in the ability of a model to simulate the MJO. The convective initiation of MJO has drawn considerable attention in recent years, and was a primary focus of the DYNAMO (see Ling et al., 2014b for abbreviation) field campaign (2011–2012). However, further studies are still needed to resolve the considerable uncertainties regarding the mechanisms that underlie the MJO.

Numerical simulations are an important resource for understanding the mechanisms behind tropical ISO and the MJO; however, AGCMs still fail to simulate many of the observed features of these phenomena. The choice of convective parameterization appears to be one of the most important factors in determining whether a model is able to simulate a realistic MJO. It is critical that diabatic heating profiles simulated by the convection scheme peak in the middle and lower troposphere. This distribution of diabatic heating facilitates strong upward motion and low-level moisture convergence, and establishes favorable conditions for the generation and development of deep convection.

Tropical ISO and the MJO evidently interact with ENSO, especially over the equatorial western Pacific. Strong MJO can induce westerly wind bursts over the western Pacific and excite oceanic Kelvin waves that favor the onset and development of El Niño. Composite analysis indicates that MJO activity is typically strong during the boreal spring preceding an El Niño event. Interannual variability in the MJO can also affect the onset of El Niño via the response of the air-sea coupled system. The mature phase of El Niño suppresses MJO activity. The relationships between MJO activity and different types of El Niño are different. Further studies will be required to better characterize the relationships between ENSO and the MJO.

Tropical ISO and their associated circulation patterns have important influences on TC activity in the western Pacific. Approximately twice as many TCs form in the northwestern Pacific during strong MJO events relative to weak MJO events. Similarly, approximately twice as many TCs form in the northwestern Pacific during the Pacific phase of MJO relative to the Indian Ocean phase of the MJO. The MJO also modulates the locations of TC genesis in the northwestern Pacific. The locations of TC genesis are generally confined to the western Pacific region south of 20°N during the Indian Ocean phase of the MJO, but extend northward to 30°N during the Pacific phase of the MJO. These two phases of the MJO are characterized by obvious differences in the distributions of the large-scale circulation, sea surface pressure, the ITCZ, vertical motion, and convective heating. The Indian Ocean phase is associated with positive anomalies in sea surface pressure, large vertical wind shear, negative anomalies in convective heating, and weak vertical motion over the northwestern Pacific. These conditions inhibit the genesis and development of TCs over the northwestern Pacific. By contrast, the Pacific phase is associated with negative anomalies in sea surface pressure, small vertical wind shear, positive anomalies in convective heating, and strong vertical motion over the northwestern Pacific. These conditions favor TC genesis over the northwestern Pacific.

ISO impacts TCs via the formation of LFC and LFAC circulation anomalies in the lower troposphere. The genesis locations for five typical TC tracks in the western Pacific all have close relationships with low-frequency circulation patterns at 850 hPa. The orientation of the belt of low-frequency cyclonic vorticity at the time of TC genesis is a good predictor of subsequent TC movement. All five TC track types are also associated with an anomalous LFAC at 200 hPa. The airflow along the south and west sides of this LFAC is also a good predictor of the TC track. The direction of the airflow along the south and west sides of the LFAC and the spatial extent of the LFAC both vary among different TC track types.

Tropical ISO activity (including the MJO) has a significant impact on the onset and variability of the SCS and EA summer monsoons. The onsets of the SCS and Indian summer monsoons are both associated with stronger tropical ISO; however, these two monsoon systems have different relationships with ISO. ISO activity over the SCS and its adjacent regions plays an important role in determining the strength of the EA summer monsoon, with strong ISO activity indicating a strong monsoon. Conversely, strong ISO activity corresponds to a weak Indian summer monsoon, and vice versa. Precipitation over China is closely related to tropical ISO activity, particularly the MJO.

The study of tropical ISO (including the MJO) remains a hot scientific topic with a number of unresolved issues. Ongoing research focuses on several areas, including the numerical simulation and forecasting of tropical ISO, the influences of tropical ISO on weather and climate (especially the role of ISO in 15–30-day extended forecasts), the interactions between tropical ISO and ENSO, and the physical mechanisms behind the convective initiation of the MJO over the western equatorial Indian Ocean.

Several other items are worthy of special attention. First, tropical ISO is the most important component of the low-frequency variability in the tropical atmosphere, but quasi-biweekly (10–20-day) oscillations also contribute. The structures, activity, and mechanisms of ISO and quasi-biweekly oscillations are significantly different. As a consequence, quasi-biweekly oscillation should not be treated as tropical ISO, and low-frequency oscillations should not be treated in a uniform way. Second, the MJO is an important and well-known example of tropical ISO. The MJO refers specifically to an eastward-propagating ISO near the equator identified in the 1970s. ISO with characteristics that differ from those of the MJO (especially with respect to zonal propagation) exists in the subtropics. Therefore, the MJO and tropical ISO should not be treated as synonymous or interchangeable. Third, the convective initiation of the MJO has recently drawn considerable attention. The convective MJO signal generally initiates over the western equatorial Indian Ocean, and then propagates eastward before disappearing around the dateline. The MJO activity over the Indian Ocean and the western Pacific can be well represented by the associated convection; however, Madden and Julian (1971, 1972) showed that the MJO has a planetary scale. The convection associated with the Indian Ocean and western Pacific MJO is only a part of the MJO structure, and does not represent the full characteristics of the MJO.

REFERENCES

Bai Xuxu, Li Chongyin, Tan Yanke, et al., 2011: Analysis of the Madden–Julian oscillation impacts on the spring rainfall in East China. *J. Trop. Meteor.*, **27**, 814–822. (in Chinese)

Barlow, M., M. Wheeler, B., Luyon, et al., 2005: Modulation of daily precipitation over Southwest Asia by the Madden–Julian oscillation. *Mon. Wea. Rev.*, **133**, 3579–3594.

Bond, N. A., and G. A. Vecchi, 2003: The influence of the Madden–Julian oscillation on precipitation in Oregon and Washington. *Wea. Forecasting*, **18**, 600–613.

Bosilovich, M., S. Schubert, G. Kim, et al., 2006: NASA's Modern Era Retrospective-Analysis for Research and Applications (MERRA). U.S. CLIVAR Variations, No. 4, International CLIVAR Project Office, Southampton, United Kingdom, 5–8.

Carr, L. E. III, and R. L. Elsberry, 1995: Monsoonal interactions leading to sudden tropical cyclone track changes. *Mon. Wea. Rev.*, **123**, 265–290.

Cha Jing and Luo Dehai, 2011: The impact of the stratiform heating on Madden–Julian oscillation. *Chinese J. Atmos. Sci.*, **35**, 657–666. (in Chinese)

Chang, C. P., 1977: Viscous internal gravity wave and low-frequency oscillation in the tropics. *J. Atmos. Sci.*, **34**, 901–910.

Chen Guanghua and Huang Ronghui, 2009: Dynamical effects of low frequency oscillation on tropical cyclogenesis over the western North Pacific and the physical mechanisms. *Chinese J. Atmos. Sci.*, **33**, 205–214. (in Chinese)

Dong Min and Li Chongyin, 2007: Some progress in the simulation study of the intraseasonal oscillation of the tropical atmosphere. *Chinese J. Atmos. Sci.*, **31**, 1113–1122. (in Chinese)

Dunkerton, T. T., 1983: A nonsymmetrical equatorial inertial in stability. *J. Atmos. Sci.*, **40**, 807–813.

Duffy, P. B., B. Govindasamy, J. P. Iorio, et al., 2003: High-resolution simulations of global climate. Part 1: Present climate. *Climate Dyn.*, **21**, 371–390.

Hall, J. D., A. J. Matthews, and D. J. Karoly, 2001: The modulation of tropical cyclone activity in Australian region by the Madden–Julian oscillation. *Mon. Wea. Rev.*, **129**, 2970–2982.

Harr, P. A., and R. L. Elsberry, 1991: Tropical cyclone track characteristics as a function of large-scale circulation anomalies. *Mon. Wea. Rev.*, **119**, 1448–1468.

Hayashi, Y., and D. G. Golder, 1986: Tropical intraseasonal oscillation appearing in a GFDL general circulation model an FGGE data. Part 1: Phase propagation. *J. Atmos. Sci.*, **45**, 3058–3067.

He Yihua, Wang Xiaoling, and Jin Qi, 2006: The preliminary analysis for the impact of intraseasonal oscillation of the tropical convection over South China Sea on the droughts and floods of Changjiang and Huaihe River basin. *J. Trop. Meteor.*, **22**, 259–264. (in Chinese)

Hendon, H. H., B. Liebmann, M. E. Newman, et al., 2000: Medium range forecasts errors associated with active episodes of the Madden–Julian oscillation. *Mon. Wea. Rev.*, **128**, 69–85.

——, M. Wheeler, and C. Zhang, 2007: Seasonal dependence of the MJO–ENSO relationship. *J. Climate*, **20**, 531–543.

Hu Chunhong, Duan Yihong, Yu Hui, et al., 2005: Diagnostic analysis of the rapid change in tropical cyclone intensity before landfall in South China. *J. Trop. Meteor.*, **21**, 377–382. (in Chinese)

Goswami, B. N., and R. S. A. Mohan, 2001: Intraseasonal oscillations and interannual variability of the Indian summer monsoon. *J. Climate*, **14**, 1180–1198.

——, R. S. Ajayamohan, P. K. Xavier, et al., 2003: Clustering of synoptic activity by Indian summer monsoon intraseasonal oscillations. *Geophys. Res. Lett.*, **30**, 1431, doi: 10.1029/2002GL016734.

Gregory, D., R. Kershaw, and P. M. Inness, 1997: Parameterrization of momentum transport by convection. II: Tests in single-column and general circulation models. *Quart. J. Roy. Meteor. Soc.*, **123**, 1153–1183.

Gushchina, D., and B. Dewitte, 2012: Intraseasonal tropical atmospheric variability associated with the two flavors of El Niño. *Mon. Wea. Rev.*, **140**, 3669–3681.

Inness, P. M., and D. Gregory, 1997: Aspects of the intraseasonal oscillation simulated by the Hadley Centre Atmosphere Model. *Climate Dyn.*, **13**, 441–458.

Jeong, J. H., B. M. Kim, C. H. Ho, et al., 2008: Systematic variation in winter-time precipitation in East Asia by MJO-Induced extratropical vertical motion. *J. Climate*, **21**, 788–801.

Jia, X. L., C. Y. Li, N. Zhou, et al., 2010: The MJO in an AGCM with three different cumulus parameterization schemes. *Dyn. Atmos. Oceans*, **49**, 141–163.

Jia Xiaolong and Li Chongyin, 2007a: Seasonal variations of the tropical intraseasonal oscillation and its reproduction in SAMIL-R42L9. *J. Trop. Meteor.*, **23**, 217–228. (in Chinese)

—— and ——, 2007b: Sensitivity of numerically simulated tropical intraseasonal oscillation to cumulus schemes. *Acta Meteor. Sinica*, **65**, 837–855. (in Chinese)

——, ——, Ling Jian, et al., 2008: Impacts of the GCM's resolution on the MJO simulation. *Adv. Atmos. Sci.*, **25**, 139–156.

——, ——, and ——, 2009: Impacts of cumulus parameterization and resolutions on the MJO simulation. *J. Trop. Meteor.*, **25**, 1–12. (in Chinese)

—— and Liang Xiaoyun, 2011: Possible impacts of the MJO on the severe ice-snow weather in November of 2009 in China. *J. Trop. Meteor.*, **27**, 639–648. (in Chinese)

——, Chen Lijuan, Ren Fumin, et al., 2011: Impacts of the MJO on winter rainfall and circulation in China. *Adv. Atmos. Sci.*, **28**, 521–533.

Jones, C., 2000: Occurrence of extreme precipitation events in California and relationships with the Madden–Julian oscillation. *J. Climate*, **13**, 3576–3587.

——, D. E. Waliser, J. K. Schemm, et al., 2000: Prediction skill of the Madden–Julian oscillation in dynamical extended range forecasts. *Climate Dyn.*, **16**, 273–289.

Kapur, A., C. Zhang, J. Zavala-Garay, et al., 2011: Role of stochastic forcing in ENSO in observations and a coupled GCM. *Climate Dyn.*, **38**, 87–107.

Kim, D., K. Sperber, W. Stern, et al., 2009: Application of MJO simulation diagnostics to climate models. *J. Climate*, **22**, 6413–6436.

Krishinamurti, T. N., and D. Subrahmanyam, 1982: The 30–50-day mode at 850 mb during MONEX. *J. Atmos. Sci.*, **39**, 2088–2095.

Lau, K. M., and P. H. Chan, 1985: Aspects of the 40–50-day oscillation during the northern winter as inferred from outgoing longwave radiation. *Mon. Wea. Rev.*, **113**, 1354–1367.

——, and L. Peng, 1987: Origin of low-frequency (intraseasonal) oscillations in the tropical atmosphere. Part I: Basic theory. *J. Atmos. Sci.*, **44**, 950–972.

Li, C. Y., X. L. Jia, J. Ling et al., 2009: Sensitivity of MJO simulations to diabatic heating profiles. *Climate Dyn.*, **32**, 167–187.

Li Chongyin, 1983: Convective condensation heating and unstable mode. *Chinese J. Atmos. Sci.*, **7**, 260–268. (in Chinese)

——, 1984: Effects of cumulus friction on the formation and maintenance of the ITCZ. *Tropical Oceanology*, **3**, 22–31. (in Chinese)

——, 1985: Actions of summer monsoon troughs (ridges) and tropical cyclones over South Asia and the moving CISK mode. *Sci. China (Ser. B)*, **15**, 668–675. (in Chinese)

——, 1989: Frequent activities of stronger aerotroughs in East Asia in wintertime and the occurrence of the El Niño event. *Sci. China (Ser. B)*, **32**, 976–985.

——, 1990: Interaction between anomalous winter monsoon in East Asia and El Niño events. *Adv. Atmos. Sci.*, **7**, 36–46.

——, 1991: *Low Frequency Oscillation in the Atmosphere*. China Meteorological Press, Beijing, 310 pp. (in Chinese)

——, 1993: A further inquiry on the mechanism of 30–60-day oscillation in the tropical atmosphere. *Adv. Atmos. Sci.*, **10**, 41–53.

——, 1996: Further studies on evaporation-wind feedback. *J. Trop. Meteor.*, **12**, 193–199. (in Chinese)

—— and Zhou Yaping, 1994: Relationship between intraseasonal oscillation in the tropical atmosphere and ENSO. *Chinese J. Geophys.*, **37**, 213–223. (in Chinese)

—— and Liao Qinghai, 1998: The exciting mechanism of tropical intraseasonal oscillation to El Niño event. *J. Trop. Meteor.*, **14**, 113–121. (in Chinese)

——, Long Zhenxia, and Zhang Qingyun, 2001: Strong/weak summer monsoon activity over the South China Sea and atmospheric intraseasonal oscillation. *Adv. Atmos. Sci.*, **18**, 1146–1160.

——, Cho Han-Ro, Wang Jough-Tai, 2002: CISK Kelvin wave with evaporation-wind feedback and air-sea interaction—A further study of tropical intraseasonal oscillation mechanism. *Adv. Atmos. Sci.*, **19**, 379–390.

——, Long Zhenxia, and Mu Mingquan, 2003: Atmospheric intraseasonal oscillation and its important effect. *Chinese J. Atmos. Sci.*, **27**, 518–535. (in Chinese)

——, Ling Jian, Jia Xiaolong, et al., 2007: Numerical simulation and comparison study of the atmospheric intraseasonal oscillation. *Acta Meteor. Sinica*, **21**, 1–8.

——, Mu Mu, Zhou Guangqing, et al., 2008: Mechanism and prediction studies of the ENSO. *Chinese J. Atmos. Sci.*, **32**, 761–781. (in Chinese)

Li Wei and Yu Yongqiang, 2001: Intraseasonal oscillation in a coupled general circulation model. *Chinese J. Atmos. Sci.*, **25**, 118–132. (in Chinese)

Liang Ping and Ding Yihui, 2012: Extended range forecast experiment based on intraseasonal oscillation. *Chinese J. Atmos. Sci.*, **36**, 102–116. (in Chinese)

Liebmann, B., H. H. Hendon, and J. D. Glick, 1994: The relationship between the tropical cyclones of the western Pacific and Indian Oceans and the Madden–Julian oscillation. *J. Meteor. Soc. Japan*, **72**, 4012–411.

Lin Ailan, Liang Jianyin, and Li Chunhui, 2005: Spectral variation characteristics of the South China Sea summer monsoon convection intraseasonal oscillation. *J. Trop. Meteor.*, **21**, 542–548. (in Chinese)

——, Li Chunhui, Gu Dejun, et al., 2013: Impact of tropical intraseasonal oscillations on the precipitation of Guangdong in June. *J. Trop. Meteor.*, **29**, 353–363. (in Chinese)

Ling, J., and C. Zhang, 2011: Structure evolution in heating profiles of the MJO in global reanlyses and TRMM retrievals. *J. Climate*, **24**, 825–842.

——, ——, and P. Bechtold, 2013b: Large-Scale preconditions for MJO and non-MJO convective initiation over the tropical Indian Ocean. *J. Atmos. Sci.*, **70**, 2696–2712.

——, C. Li, W. Zhou, et al., 2014a: To begin, or not to begin?—A case study on MJO initiation problem. *Theor. Appl. Climatol.*, **115**, 231–241.

——, P. Bauer, P. Bechtold, et al., 2014b: Global vs. local MJO forecast skill of the ECMWF model during DYNAMO. *Mon. Wea. Rev.*, **142**, 2228–2247, doi:10.1175/MWR-D-13-00292.1.

Ling Jian, Li Chongyin, and Jia Xiaolong, 2009: Impacts of cumulus momentum transport on MJO simulation. *Adv. Atmos. Sci.*, **26**, 864–876.

——, ——, Zhou Wen, et al., 2013a: Effect of boundary layer latent heating on MJO simulations. *Adv. Atmos. Sci.*, **30**, 101–115.

—— and ——, 2014: Impact of convective momentum transport by deep convection on simulation of tropical intraseasonal oscillation. *J. Ocean Univ. China,* **13**, 717–727.

Liu Qinyu, Liu Yanyun, and Huang Fei, 2008: A study of the response of El Niño/Southern oscillation to external forcing in the tropical western Pacific. *J. Ocean Univ. China*, **38**, 345–351. (in Chinese)

Long Zhenxia and Li Chongyin, 2002: Interannual variation of tropical atmospheric 30–60-day low-frequency oscillation and ENSO cycle. *Chinese J. Atmos. Sci.*, **26**, 51–62. (in Chinese)

Lü Junmei, Ju Jianhua, Ren Juzhang, et al., 2012: The influence of the Madden–Julian oscillation activity anomalies on Yunnan's extreme drought of 2009–2010. *Sci. China Earth Sci.*, **42**, 599–613. (in Chinese)

Madden, R. A., and P. R. Julian, 1971: Detection of a 40–50-day oscillation in the zonal wind in the tropical Pacific. *J. Atmos. Sci.*, **28**, 702–708.

——, and ——, 1972: Description of global scale circulation cells in the tropics with 40–50-day period. *J. Atmos. Sci.*, **29**, 1109–1123.

——, and ——, 1994: Observations of the 40–50-day tropical oscillation—A review. *Mon. Wea. Rev.*, **122**, 814–837.

Maloney, E. D., and D. L. Hartmann, 2000a: Modulation of hurricane activity in the Gulf of Mexico by the Madden–Julian oscillation. *Science*, **287**, 2002–2004.

——, and ——, 2000b: Modulation of eastern North pacific hurricanes by the Madden–Julian oscillation. *J. Climate*, **13**, 1451–1465.

——, and ——, 2001: The sensitive of intraseasonal variability in the NCAR CCM3 to changes in convection parameterization. *J. Climate*, **14**, 2015–2034.

Manabe, S., and R. F. Strickler, 1964: Thermal equilibrium of the atmosphere with a convective adjustment. *J. Atmos. Sci.*, **21**, 361–385.

Marshall, A. G., O. Alves, and H. H. Hendon, 2009: A coupled GCM analysis of MJO activity at the onset of El Niño. *J. Atmos. Sci.*, **66**, 966–983.

Mu Mingquan and Li Chongyin, 2000: On the outbreak of South China sea summer monsoon in 1998 and activity of atmospheric intraseasonal oscillation. *Climatic Environ. Res.*, **5**, 375–387. (in Chinese)

Murakami, T., T. Nakazawa, J. He, 1984: On the 40–50-day oscillations during the 1979 Northern Hemisphere summer. I: Phase propagation. *J. Meteor. Soc. Japan*, **62**, 440–468.

——, L. X. Chen, and A. Xie, 1986: Relationship among seasonal cycles, low-frequency oscillations, and transient disturbances as revealed from outgoing longwave radiation data. *Mon. Wea. Rev.*, **114**, 1456–1465.

Neelin, J. D., J. David, M. Isaac, et al., 1987: Evaporation-wind feedback and low-frequency variability in the tropical atmosphere. *J. Atmos. Sci.*, **44**, 2341–2348.

Nordeng, T. E., 1994: Extended versions of the convective parameterization scheme at ECMWF and their impact on the mean and transient activity of the model in the Tropics. ECMWF Research Department, Technic Memo 206, October 1994. European Center for Medium Range Weather Forecasts, Reading, UK, 41 pp.

Pan Jin, Li Chongyin, and Song Jie, 2010: The modulation of Madden–Julian oscillation on typhoons in the northwestern Pacific Ocean. *Chinese J. Atmos. Sci.*, **34**, 1059–1070. (in Chinese)

Peng Yuehua, Duan Wansuo, and Xiang Jie, 2011: Effect of stochastic MJO forcing on ENSO predictability. *Adv. Atmos. Sci.*, **28**, 1279–1290.

Qi, Y. J., R. H. Zhang, T. Li, et al., 2008: Interactions between the summer mean monsoon and the intraseasonal oscillation in the Indian monsoon region. *Geophys. Res. Lett.*, **35**, L17704, doi: 10.1029/2008GL034517.

Qi Yanjun, Zhang Renhe, Li Tim, et al., 2009: Impacts of intraseasonal oscillation on the onset and interannual variation of the Indian summer monsoon. *Chin. Sci. Bull.*, **54**, 880–884.

Richard, B. N., J. H. Richter, and M. Jochum, 2008: The impact of convection on ENSO: From a delayed oscillator to a series of events. *J. Climate*, **21**, 5904–5924.

Rong, X. Y., R. H. Zhang, T. Li, et al., 2011: Upscale feedback of high-frequency winds to ENSO. *Quart. J. Roy. Meteor. Soc.*, **137**, 894–907.

Roundy, P. E., and J. R. Kravitz, 2009: The association of the evolution of intraseasonal oscillations to ENSO phase. *J. Climate*, **22**, 381–395.

Saha, S., and Coauthors, 2010: The NCEP climate forecast system reanalysis. *Bull. Amer. Meteor. Soc.*, **91**, 1015–1057.

Seiki, A., Y. N. Takayabu, K. Yoneyama, et al., 2009: The Oceanic response to the Madden–Julian oscillation and ENSO. *SOLA*, **5**, 93–96.

Slingo, J. M., and R. A. Madden, 1991: Characterictics of the tropical intraseasonal oscillation in the NCAR community climate model. *Quart. J. Roy. Meteor. Soc.*, **117**, 1129–1169.

——, K. R. Sperber, J. S. Boyle, et al., 1996: Intraseasonal oscillations in 15 atmospheric general circulation models: Results from an AMIP diagnostic subproject. *Climate Dyn.*, **12**, 325–357.

Sobel, A. H., and E. D. Maloney, 2000: Effect of ENSO and the MJO on western North Pacific tropical cyclones. *Geophys. Res. Lett.*, **27**, 1739–1742.

Sperber, K. R., 2004: Madden–Julian variability in NCAR CAM 2.0 and CCSM2.0. *Climate Dyn.*, **23**, 259–278.

Sun Guowu, Li Zhenkun, Xin Fei, et al., 2013: Low-frequency synoptic map: New method for extended-range forecasting. *Chinese J. Atmos. Sci.*, **37**, 945–954. (in Chinese)

Sun Zhang, Mao Jiangyu, and Wu Guoxiong, 2009: Influences of intraseasonal oscillation on the clustering of tropical cyclone activity over the western North Pacific during boreal summer. *Chinese J. Atmos. Sci.*, **33**, 950–958. (in Chinese)

Tang, Y., and B. Yu, 2008: An analysis of nonlinear relationship between the MJO and ENSO. *J. Meteor. Soc. Japan*, **86**, 867–881.

Tian Hua, Li Chongyin, and Yang Hui, 2010a: Modulation of typhoon tracks over the western North Pacific by the intraseasonal oscillation. *Chinese J. Atmos. Sci.*, **34**, 559–579. (in Chinese)

——, ——, and ——, 2010b: Modulation of typhoon genesis over the western North Pacific by intraseasonal oscillation. *J. Trop. Meteor.*, **26**, 283–292. (in Chinese)

Tiedtke, M., 1989: A comprehensive mass flux scheme for cumulus parameterization in large-scale models. *Mon. Wea. Rev.*, **117**, 1779–1800.

Tung, W. W., and M. Yanai, 2002: Convective momentum transport observed during the TOGA COARE

IOP. Part II: Case studies. *J. Atmos. Sci.*, **59**, 2535–2549.

Wang, B., 1988: Dynamics of tropical low-frequency waves–An analysis of the moist Kelvin wave. *J. Atmos. Sci.*, **45**, 2051–2065.

——, and X. Xu, 1997: Northern Hemisphere summer monsoon singularities and climatological intraseasonal oscillation. *J. Climate*, **10**, 1071–1085.

Wang, W. Q., and M. E. Schlesinger, 1999: The dependence on convection parameterization of the tropical intraseasonal oscillation simulated by the UIUC 11-layer atmospheric GCM. *J. Climate*, **12**, 1423–1457.

Wheeler, M. C., and H. H. Hendon, 2004: An all-season real-time multivariate MJO index: Development of an index for monitoring and prediction. *Mon. Wea. Rev.*, **132**, 1917–1932.

——, ——, S. Cleland, et al., 2008: Impacts of the Madden–Julian oscillation on Australian rainfall and circulation. *J. Climate*, **22**, 1482–1498.

Wu Junjie, Yuan Zhuojian, Qian Yukun, et al., 2009: The role of intraseasonal oscillation in the southern-China snowstorms during January 2008. *J. Trop. Meteor.*, **25**, 103–111. (in Chinese)

Wu, X., L. Deng, X. Song, et al., 2007: Coupling of convective momentum transport with convective heating in global climate simulations. *J. Atmos. Sci.*, **64**, 1334–1349.

Yang Hui and Li Chongyin, 2003: The relation between atmospheric intraseasonal oscillation and summer severe flood and drought in the Jianghuai River basin. *Adv. Atoms. Sci.*, **20**, 540–553.

Yang Jing, Bao Qing, Wang Xiaocong, et al., 2012: The tropical intraseasonal oscillation in SAMIL coupled and uncoupled general circulation models. *Adv. Atmos. Sci.*, **29**, 529–543.

Yuan Yuan, Yang Hui, and Li Chongyin, 2012: Study of El Niño events of different types and their potential impact on the following summer precipitation in China. *Acta Meteor. Sinica*, **70**, 467–478. (in Chinese)

Zavala-Garay, J., and C. Zhang, 2004: The linear response of ENSO to the Madden–Julian oscillation. *J. Climate*, **17**, 2441–2459.

——, ——, A. M. Moore, et al., 2008: Sensitivity of hybrid ENSO models to unresolved atmospheric variability. *J. Climate*, **21**, 3704–3721.

Zhang, C., and J. Gottschalck, 2002: SST anomalies of ENSO and the Madden–Julian oscillation in the equatorial Pacific. *J. Climate*, 15, 2429–2445.

——, and J. Ling, 2012: Potential vorticity of the Madden–Julian oscillation. *J. Atmos. Sci.*, **69**, 65–78.

Zhang, C. D., 2005: Madden–Julian oscillation. *Rev. Geophys.*, **43**, doi: 10.1029/2004RG000158.

Zhang, G. J., and N. A. McFarlane, 1995: Sensitivity of climate simulation to the parameterization of cumulus convection in the Canadian Climate Centre General Circulation Model. *Atmos. Ocean*, **33**, 407–446.

Zhang, L., B. Wang, and Q. Zeng, 2009: Impact of the Madden–Julian oscillation on summer rainfall in Southeast China. *J. Climate*, **22**, 201–216.

Zhang Lina, Lin Pengfei, Xiong Zhe, et al., 2011: Impact of the Madden–Julian oscillation on pre-flood season precipitation in South China. *Chinese J. Atmos. Sci.*, **35**, 560–570. (in Chinese)

Zhou, W., and J. C. L. Chan, 2005: Intraseasonal oscillations and the South China Sea summer monsoon onset. *Int. J. Climatol.*, **25**, 1585–1609.

Zhu Congwen, T. Nakazawa, and Li Jianping, 2004: Modulation of tropical depression/cyclone over the Indian–western Pacific oceans by Madden–Julian oscillation. *Acta Meteor. Sinica*, **62**, 42–50. (in Chinese)

Zhu Lijuan, Wang Yafei, and Yin Zhicong, 2013: Relationship between tropical cyclone activity over the South China sea and tropical ISO propagation. *J. Trop. Meteor.*, **29**, 737–748. (in Chinese)